Attosecond Pulse Shaping around a Cooper Minimum

S. B. Schoun,* R. Chirla, J. Wheeler, C. Roedig, P. Agostini, and L. F. DiMauro
Department of Physics, The Ohio State University, Columbus, Ohio 43210, USA

K. J. Schafer and M. B. Gaarde†
Department of Physics and Astronomy, Louisiana State University, Baton Rouge, Louisiana 70803, USA

(Received 18 September 2013; published 14 April 2014)

High harmonic generation (HHG) is used to measure the spectral phase of the recombination dipole matrix element (RDM) in argon over a broad frequency range that includes the $3p$ Cooper minimum (CM). The measured RDM phase agrees well with predictions based on the scattering phases and amplitudes of the interfering s- and d-channel contributions to the complementary photoionization process. The reconstructed attosecond bursts that underlie the HHG process show that the derivative of the RDM spectral phase, the group delay, does not have a straightforward interpretation as an emission time, in contrast to the usual attochirp group delay. Instead, the rapid RDM phase variation caused by the CM reshapes the attosecond bursts.

DOI: 10.1103/PhysRevLett.112.153001 PACS numbers: 32.70.-n, 42.65.Ky, 42.65.Re

One signature of atomic structure, first discussed by Cooper [1], is a local minimum in the photoionization (PI) probability at a specific photon energy. This Cooper minimum (CM) is caused by a sign change, equivalent to a π phase jump, in the bound-free transition dipole of one angular momentum channel. The CM has been extensively studied using traditional photoionization spectroscopy, but the phase of the total transition dipole is not directly accessible, although it strongly influences the measured electron angular distribution and spin polarization [2,3]. The time-domain consequences of the CM in PI are illustrated as path (1) in Fig. 1(a): a smooth ultrafast extreme-ultraviolet (XUV) pulse with sufficient bandwidth and proper photon energy produces an outgoing electron wave packet (EWP) inscribed with the CM hole [4,5]. Experimental reconstruction of such an outgoing EWP, however, requires complete knowledge of the amplitude and phase [5], and to date no measurement has demonstrated the double-peaked structure illustrated in Fig. 1(a).

In high harmonic generation (HHG) the inverse process of broadband PI takes place: an EWP, promoted and accelerated in the continuum by an intense optical pulse, returns to the core and gives rise to emission of XUV radiation through photorecombination, as illustrated by path (2) in Fig. 1(b). The propagation of the EWP is determined by the laser wavelength and intensity, while the recombination process has been shown to be independent of the laser [6–10]. The EWP thereby acts as a self-probe of the laser-free complex recombination dipole matrix element (RDM). A measurement of the emitted XUV radiation can provide access to both the amplitude and phase of the RDM; thus, it can be used to study structural features of the generating atom or molecule [10–14], and in particular the CM. As illustrated by path (3) in Fig. 1(b), the time domain consequences of the CM amplitude and phase modulation are such that a smooth returning EWP will be shaped into a structured XUV time profile.

In this Letter, we investigate the phase modification in the high harmonic emission induced by the $3p$ Cooper minimum of argon over a wide spectral range. In the experiment, the derivative of the spectral phase, the group delay (GD), is measured using the resolution of attosecond beating by interference of two-photon transitions (RABBITT) method [15,16]. The measured phase and amplitude are compared with both an illustrative simple

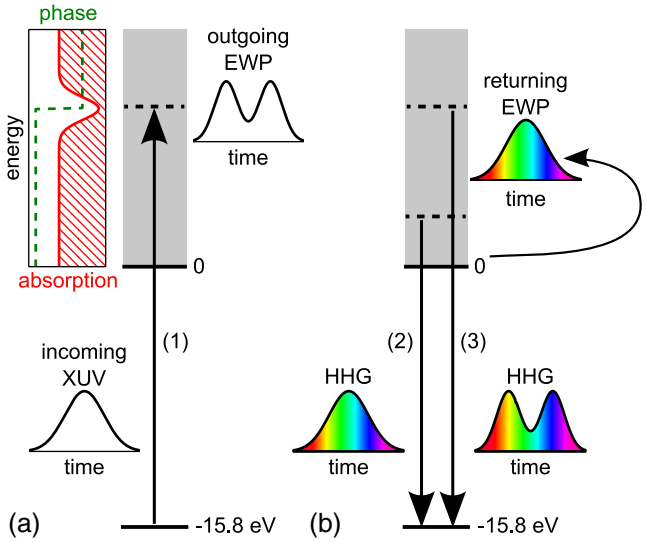

FIG. 1 (color online). Energy level diagram and time-domain picture of EWPs and broadband XUV pulses in (a) photoionization and (b) photorecombination in HHG in the vicinity of a Cooper minimum. See text for the discussion of paths (1), (2), and (3).

model and a more comprehensive calculation using numerical solutions of the Schrödinger and Maxwell wave equations. Previous studies [7,8,17,18] have observed the CM feature in the frequency spectrum of the emitted harmonic comb, but not the spectral phase. In principle, RABBITT can access the RDM phase, although knowledge of other phase contributions is necessary. The leading contribution is a single-atom effect caused by the accumulated phase of the field-driven rescattering EWP [19,20], the so-called attochirp. There are also several macroscopic contributions involving the propagation through the argon source, spectral filters, and the RABBITT detection gas. However, our results unequivocally establish that direct measurement of the RDM phase near a CM can be extracted from RABBITT.

Our work also allows us to establish the relation between the measured GD and the time structure of the XUV emission in the presence of an (anti)resonance, and to illustrate the limitations of interpreting the GD as a time delay [21,22]. Typically in HHG, the GD is appropriately interpreted as the emission time of different frequencies in the harmonic spectrum, as depicted by path (2) in Fig. 1(b) [19,20,23]. Near a CM, however, it is misleading to interpret the GD as only a frequency-dependent time delay; rather, as we will show, the rapid phase variation leads to a reshaping of the temporal envelope of the broadband XUV light. This is depicted as the doublet in path (3) of Fig. 1(b). The same caveat applies to studies of time delay in PI using attosecond pulses [21,22]. Near an (anti)resonance, the EWP created by an attosecond pulse will be similarly reshaped, and the GD takes on a richer interpretation.

In the experiment, the HHG source utilizes a tunable optical parametric amplifier to generate 65 fs, midinfrared (MIR) pulses at the wavelengths of 1.3 and 2.0 μm at a 1 kHz repetition rate. The laser is focused ~1–2 mm in front of the argon nozzle to phase match the short trajectory, and, in combination with an aperture in the far field, to minimize long trajectory harmonic contributions. A thin argon jet (< 0.5 mm, $1–5 \times 10^{18}$ cm^{-3}) provides good phase matching while minimizing neutral atom dispersion.

The RABBITT apparatus is a Mach-Zehnder interferometer design. The XUV propagates in one arm and a small amount of the fundamental MIR light propagates in the other. The pulses are recombined with a variable relative delay, spatially overlapped, and focused into a magnetic bottle electron spectrometer (MBES) [24]. Neon gas introduced into the MBES is the photoionization detector. Information about the XUV spectral phase is encoded in the delay dependent oscillation of the two-color sidebands in the neon photoelectron energy spectrum. In this Letter, the use of the longer wavelength MIR sources provides advantages over conventional 0.8 μm drive lasers. First, the harmonic cutoff energy scales quadratically with the drive laser wavelength [25]; consequently, the harmonic spectral plateau extends well beyond the argon CM at 50 eV photon energy and ensures a linear dependence in the attochirp GD near the CM [26]. Second, the smaller photon energy provides a finer sampling of the CM amplitude and phase.

Figure 2 shows raw experimental data for the harmonic yield (a) and GD (b) for two different driving wavelengths, 1.3 and 2 μm. The laser intensity is estimated to be 157 and 94 TW/cm^2, respectively. Also plotted are the estimated contributions to the total measured GD that are used to retrieve the RDM contribution: the attochirp GD of the short trajectory calculated semiclassically [19,20], the macroscopic GD including neutral-atom [27,28] and

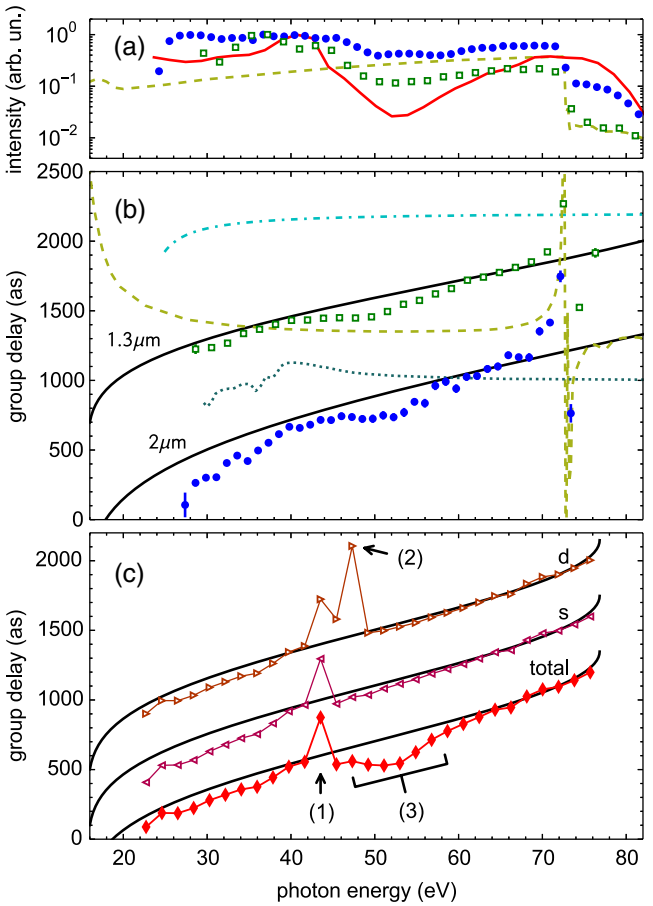

FIG. 2 (color online). (a) Raw experimental HHG yield for 1.3 μm (open squares) and 2 μm (solid circles), with estimated transmission of 0.2 μm thick Al filter (dashed line), and time-dependent Schrödinger equation (TDSE)-Maxwell's wave equation (MWE) calculation yield (solid line) for 1.3 μm. (b) Raw experimental GD measurements [same symbols as (a)] with estimated GD contributions (offset for clarity) from the Ne atomic phase delay (dash-dotted line), Al filter dispersion (dashed line), and neutral Ar dispersion for a gas density-length product of 2.5×10^{17} cm^{-2} (dotted line). (c) TDSE-MWE calculations of the total GD (diamonds) for 1.3 μm, along with the individual *s* (left triangles) and *d* contributions (right triangles) to the GD. The numbered regions are discussed in the text. In (b),(c) the attochirp GD (solid lines) is shown for reference.

aluminum filter dispersion [29,30], and the atomic phase delay [31–34] of the RABBITT detection gas [35]. The GD from plasma dispersion is small and has been neglected. After subtracting these various contributions from the total measured GD, we arrive at the main result of this Letter: the RDM group delay shown in Fig. 3(a) and, upon integration, the RDM phase in Fig. 3(b) near the CM antiresonance.

The large-scale calculations in this study are performed by solving the coupled TDSE-MWE. The MWE is solved by space marching through the harmonic gas jet, with each plane in the propagation direction having a source polarization field term calculated by numerically solving the TDSE [17,36] in the single active electron approximation. We use an ℓ-dependent pseudopotential [33] to describe the electron-core interaction. This allows us to separately calculate the major contributions to the dipole moment (and thereby the macroscopic electric field) due to transitions from continuum s and d states to the ground $3p$ state [17]. Tabulated values are used for the linear absorption and dispersion in argon [28], as these are underestimated by the pseudopotential. The GD is calculated from the radially averaged spectral phase of the macroscopic electric field [37], which is spatially filtered in the far field, as in the experiment.

The TDSE-MWE curves in Fig. 2(c) illustrate the origin of the CM group delay and the agreement with the measurement. With similar focusing conditions to the experiment, the GD is calculated assuming 130 TW/cm^2, 1.3 μm driving field focused 1 mm before the center of a 1.25 mm Ar gas jet with a density of 2.5×10^{18} cm^{-3}. The agreement of the measured and calculated total GD is good except near 44 eV photon energy (this phase jump, arrow 1, is caused by atomic dispersion; see comments in [38]). Figure 2(c) also shows the individual s and d contributions. The s channel shows a simple monotonic increase except for the same dispersion jump near 44 eV. The d-channel GD is similar, with the addition of one large jump at 48 eV (arrow 2), owing to the derivative of the π phase jump in that channel. However, the total GD is the coherent sum of both channels, which reproduces the measured CM phase over the range of 48–60 eV (region 3). Since the two channels have the same attochirp, the dipole GD can be extracted from the calculation by subtracting the s GD from the total GD [39]. The result is shown as the solid lines in Fig. 3, and is in good agreement with the experimental RDM which was extracted in a completely different manner. This provides clear evidence that RDM phases can be accurately measured using HHG.

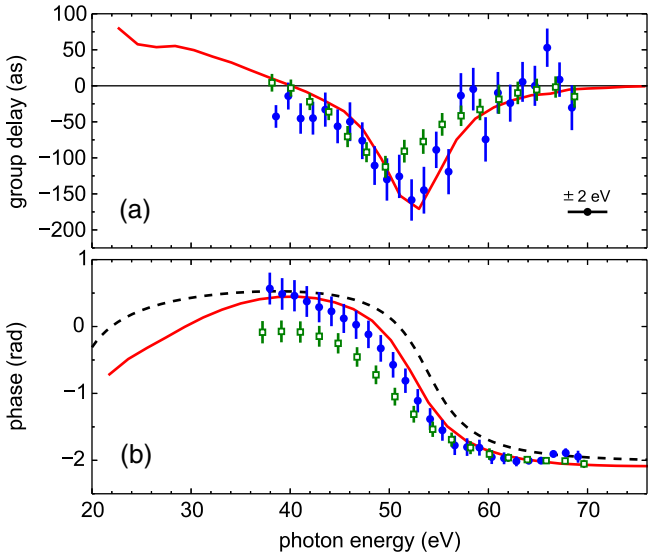

FIG. 3 (color online). Argon measurements for 1.3 μm (open squares) and 2 μm (solid circles), and TDSE-MWE calculation (solid lines) of the RDM (a) group delay and (b) phase. (b) also plots the RDM phase (dashed line) calculated with the simple model, Eq. (1). The horizontal line in (a) is the relative calibration error of the harmonic energy at the different drive wavelengths.

Figure 3(b) shows that the total RDM phase evolves by 1.8–2.6 radians over a 20 eV spectral range, even though the d-channel RDM undergoes a sharp π phase shift. Our measurements are within the range of previous calculated values of 2.4 rad [6], 2.6 rad [7], 2.1 rad [8], and 1.9 rad [40]. We note that these values should also be accessible via PI measurements using attosecond pulses.

Regardless of the complex nature of the RDM phase, we can employ a simple model to understand the important parameters that determine the phase behavior. The total dipole moment $p(\omega)$ is approximated by accounting for the relative strength, $\chi(\omega)$, and the relative scattering phase, $\xi(\omega)$, of the s and d contributions,

$$p(\omega) = s(\omega)e^{i\eta_0(\omega)}[1 + \chi(\omega)e^{i\xi(\omega)}],$$
$$\chi(\omega) = \frac{d(\omega)}{s(\omega)}, \qquad \xi(\omega) = \eta_2(\omega) - \eta_0(\omega). \tag{1}$$

We model the relative amplitude as a linear function, $\chi(\omega) = -(\omega - \omega_C)/\Delta\omega$, where $\omega_C = 48.5$ eV is the energy of the d-channel zero crossing and $1/\Delta\omega$ defines the slope, which is estimated to be $\Delta\omega = 6.6$ eV from the TDSE-MWE calculations. The scattering phases $\eta_\ell(\omega) = \sigma_\ell(\omega) + \delta_\ell(\omega)$ include the Coulomb contribution $\sigma_\ell(\omega) = \arg\{\Gamma[\ell + 1 - i/k(\omega)]\}$, where $k(\omega)$ is the electron wave number in atomic units and Γ is the gamma function, and the short range potential scattering phases ($\delta_2 = 1.4$ rad, $\delta_0 = 0$ rad), which are assumed constant.

The simple model is compared to the experiment and TDSE-MWE in Fig. 3(b), where it is seen to achieve a similar phase evolution. The model emphasizes that the phase of the total RDM is heavily influenced by the relative strength of the two channels, while the s contribution moderates and shapes the d phase jump.

We now comment on the meaning of the negative GD caused by the CM in Fig. 3(a). For a recombining EWP with a linear GD, e.g., attochirp, the GD is often interpreted

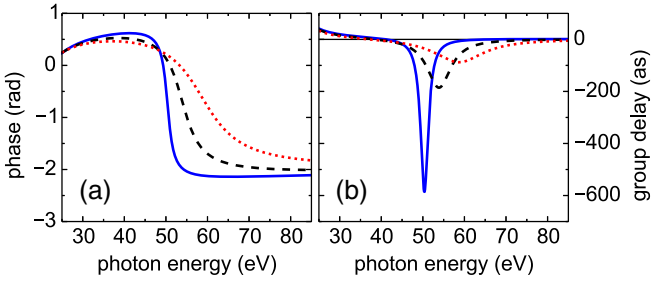

FIG. 4 (color online). Dipole (a) phase and (b) GD, calculated from the simple model in Eq. (1) for argon $3p$ with $\Delta\omega = 6.6$ eV (dashed lines), compared with an atom that has a larger or smaller relative amplitude strength, for example, $\Delta\omega = 2.2$ eV (solid lines) or $\Delta\omega = 13.2$ eV (dotted lines). Note that a small (large) $\Delta\omega$ means that the s contribution is relatively weak (strong) compared to the d contribution.

as an emission time of the XUV light [23]. However, if the GD is not linear, such as the rapid modulation near the CM, then this correspondence between GD and emission time breaks down. This is further complicated by the fact that the GD at the CM can become arbitrarily large and narrow (or small and wide) depending on the relative strength of the two channels, as illustrated by the simple model in Fig. 4. As discussed below, the effect of the CM on broadband XUV emission is not a simple time delay, but an entire reshaping of the pulse. Similarly, since the same dipole matrix element describes both recombination and ionization, one could expect that defining an ionization delay time via the group delay, as is often done [41,42], will lead to difficulties, especially if the GD is larger than the pulse width [43]. In contrast, a PI experiment performed with narrow-band XUV light would allow for a much closer correspondence [41,44].

With a measurement of the XUV spectral phase, we can now see how the presence of a CM in the dipole moment alters the shape of the emitted attosecond pulses. Figure 5(a) shows the time profile of one attosecond burst reconstructed

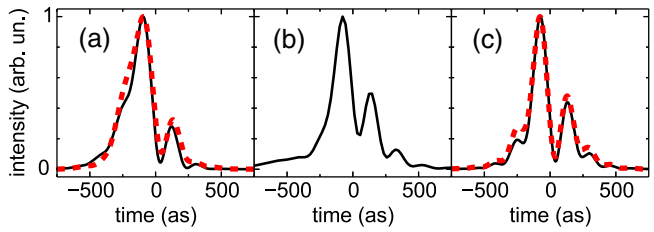

FIG. 5 (color online). Attosecond XUV time profiles reconstructed from a 24 eV spectral bandwidth centered on the CM feature, using the amplitude and phase results of the (a) 1.3 μm (solid line) and 2 μm (dashed line) experiments, (b) 1.3 μm TDSE-MWE calculations, and (c) 1.3 μm (solid line) and 2 μm (dashed line) simple model, Eq. (1), including the classical wave packet phase to match the attochirp of the experiment.

from the experimental spectral amplitude and phase. The measurements are corrected for the Al filter transmission and dispersion, as well as the RABBITT detection gas. The corresponding profile from the macroscopic electric field calculated by the TDSE-MWE is shown in Fig. 5(b) and yields excellent agreement with the experiment. Also, the simple model discussed above, when combined with the attochirp, exhibits a similar double-peaked time profile as shown in Fig. 5(c).

The structured attosecond emission shown in Fig. 5 is characteristic of the amplitude and phase modulation caused by a CM or, more generally, an (anti)resonance [45]. The beating between the frequency components on either side of the spectral minimum, which are out of phase by approximately π, produces multiple peaks in the time domain. Thus, the CM shapes the time-dependent dipole and imparts an additional amplitude modulation in the emission not found in the rescattering EWP. The same principle, but in reverse, holds for PI, as illustrated in Fig. 1(a). Broadband XUV light tuned near the CM would create an EWP that has additional structure not found in the excitation pulse [4].

In summary, the spectral phase of the RDM in argon around the $3p$ Cooper minimum has been characterized using RABBITT measurements and the phase structure imposed by the CM has been extracted.

The OSU work was supported by the DOE under Contract No. DE-FG02-04ER15614. The LSU work was supported by the NSF under Grants No. PHY-0701372 and No. PHY-1019071. Computational resources were provided by Louisiana Optical Network Initiative (www.loni.org). L. F. D. acknowledges support from the Dr. Edward and Sylvia Hagenlocker Chair.

*schoun.1@osu.edu
†gaarde@phys.lsu.edu

[1] J. W. Cooper, Phys. Rev. **128**, 681 (1962).
[2] N. A. Cherepkov, Zh. Eksp. Teor. Fiz. **65**, 933 (1973) [Sov. Phys. JETP **38**, 463 (1974)].
[3] K.-N. Huang, W. R. Johnson, and K. T. Cheng, At. Data Nucl. Data Tables **26**, 33 (1981).
[4] J. H. Hoogenraad, R. B. Vrijen, and L. D. Noordam, Phys. Rev. A **57**, 4546 (1998).
[5] V. S. Yakovlev, J. Gagnon, N. Karpowicz, and F. Krausz, Phys. Rev. Lett. **105**, 073001 (2010).
[6] A.-T. Le, T. Morishita, and C. D. Lin, Phys. Rev. A **78**, 023814 (2008).
[7] H. J. Wörner, H. Niikura, J. B. Bertrand, P. B. Corkum, and D. M. Villeneuve, Phys. Rev. Lett. **102**, 103901 (2009).
[8] C. Jin, A.-T. Le, and C. D. Lin, Phys. Rev. A **83**, 023411 (2011).
[9] M. V. Frolov, N. L. Manakov, T. S. Sarantseva, and A. F. Starace, Phys. Rev. A **83**, 043416 (2011).
[10] A.-T. Le, R. R. Lucchese, S. Tonzani, T. Morishita, and C. D. Lin, Phys. Rev. A **80**, 013401 (2009).

[11] J. Itatani, J. Levesque, D. Zeidler, H. Niikura, H. Pépin, J. C. Kieffer, P. B. Corkum, and D. M. Villeneuve, Nature (London) **432**, 867 (2004).
[12] B. K. McFarland, J. P. Farrell, P. H. Bucksbaum, and M. Gühr, Science **322**, 1232 (2008).
[13] B. K. McFarland, J. P. Farrell, P. H. Bucksbaum, and M. Gühr, Phys. Rev. A **80**, 033412 (2009).
[14] S. Haessler, J. Caillat, W. Boutu, C. Giovanetti-Teixeira, T. Ruchon, T. Auguste, Z. Diveki, P. Breger, A. Maquet, B. Carré, R. Taïeb, and P. Salières, Nat. Phys. **6**, 200 (2010).
[15] P. M. Paul, E. S. Toma, P. Breger, G. Mullot, F. Augé, P. Balcou, H. G. Muller, and P. Agostini, Science **292**, 1689 (2001).
[16] H. G. Muller, Appl. Phys. B **74**, S17 (2002).
[17] J. P. Farrell, L. S. Spector, B. K. McFarland, P. H. Bucksbaum, M. Gühr, M. B. Gaarde, and K. J. Schafer, Phys. Rev. A **83**, 023420 (2011).
[18] J. Higuet, H. Ruf, N. Thiré, R. Cireasa, E. Constant, E. Cormier, D. Descamps, E. Mével, S. Petit, B. Pons, Y. Mairesse, and B. Fabre, Phys. Rev. A **83**, 053401 (2011).
[19] S. Kazamias and P. Balcou, Phys. Rev. A **69**, 063416 (2004).
[20] K. Varjú, Y. Mairesse, B. Carré, M. B. Gaarde, P. Johnsson, S. Kazamias, R. López-Martens, J. Mauritsson, K. J. Schafer, P. Balcou, A. L'Huillier, and P. Salières, J. Mod. Opt. **52**, 379 (2005).
[21] M. Schultze, M. Fieß, N. Karpowicz, J. Gagnon, M. Korbman, M. Hofstetter, S. Neppl, A. L. Cavalieri, Y. Komninos, T. Mercouris, C. A. Nicolaides, R. Pazourek, S. Nagele, J. Feist, J. Burgdörfer, A. M. Azzeer, R. Ernstorfer, R. Kienberger, U. Kleineberg, E. Goulielmakis, F. Krausz, and V. S. Yakovlev, Science **328**, 1658 (2010).
[22] K. Klünder, J. M. Dahlström, M. Gisselbrecht, T. Fordell, M. Swoboda, D. Guénot, P. Johnsson, J. Caillat, J. Mauritsson, A. Maquet, R. Taïeb, and A. L'Huillier, Phys. Rev. Lett. **106**, 143002 (2011).
[23] Y. Mairesse, A. de Bohan, L. J. Frasinski, H. Merdji, L. C. Dinu, P. Monchicourt, P. Breger, M. Kovačev, R. Taïeb, B. Carré, H. G. Muller, P. Agostini, and P. Salières, Science **302**, 1540 (2003).
[24] P. Kruit and F. H. Read, J. Phys. E **16**, 313 (1983).
[25] J. Tate, T. Auguste, H. G. Muller, P. Salières, P. Agostini, and L. F. DiMauro, Phys. Rev. Lett. **98**, 013901 (2007).
[26] G. Doumy, J. Wheeler, C. Roedig, R. Chirla, P. Agostini, and L. F. DiMauro, Phys. Rev. Lett. **102**, 093002 (2009).
[27] K. T. Kim, K. S. Kang, M. N. Park, T. Imran, G. Umesh, and C. H. Nam, Phys. Rev. Lett. **99**, 223904 (2007).
[28] B. L. Henke, E. M. Gullikson, and J. C. Davis, At. Data Nucl. Data Tables **54**, 181 (1993).
[29] R. López-Martens, K. Varjú, P. Johnsson, J. Mauritsson, Y. Mairesse, P. Salières, M. B. Gaarde, K. J. Schafer, A. Persson, S. Svanberg, C.-G. Wahlström, and A. L'Huillier, Phys. Rev. Lett. **94**, 033001 (2005).
[30] A. D. Rakić, Appl. Opt. **34**, 4755 (1995).
[31] V. Véniard, R. Taïeb, and A. Maquet, Phys. Rev. A **54**, 721 (1996).
[32] E. S. Toma and H. G. Muller, J. Phys. B **35**, 3435 (2002).
[33] J. Mauritsson, M. B. Gaarde, and K. J. Schafer, Phys. Rev. A **72**, 013401 (2005).
[34] J. M. Dahlström, D. Guénot, K. Klünder, M. Gisselbrecht, J. Mauritsson, A. L'Huillier, A. Maquet, and R. Taïeb, Chem. Phys. **414**, 53 (2013).
[35] One additional contribution to the measured GD which has not been estimated is the effect of the energy dependence of the harmonic Gouy phases, as recently measured in Ref. [44]. We speculate that this may contribute to the poor experimental agreement with the classical wave packet group delay for harmonics below 38 eV.
[36] M. B. Gaarde, C. Buth, J. L. Tate, and K. J. Schafer, Phys. Rev. A **83**, 013419 (2011).
[37] M. B. Gaarde and K. J. Schafer, Phys. Rev. Lett. **89**, 213901 (2002).
[38] The Ar dispersion is large in the 40–45 eV region, which leads to complicated phase matching and an unstable spectral phase. In calculations where we artificially suppress linear dispersion, the phase jump in this region goes away. We note also that since this phase jump appears in both the *s*, *d*, and total GD, it cancels when we evaluate the total RDM phase.
[39] This works because the dipole GD from the *s* channel alone is nearly constant [see text surrounding Eq. (1)]. Had it not been constant, it would have to be added back in to obtain the total dipole GD.
[40] A. S. Kheifets (private communication); Phys. Rev. A **87**, 063404 (2013).
[41] J. Caillat, A. Maquet, S. Haessler, B. Fabre, T. Ruchon, P. Salières, Y. Mairesse, and R. Taïeb, Phys. Rev. Lett. **106**, 093002 (2011).
[42] J. M. Dahlström, A. L'Huillier, and A. Maquet, J. Phys. B **45**, 183001 (2012).
[43] V. V. Serov, V. L. Derbov, and T. A. Sergeeva, Phys. Rev. A **87**, 063414 (2013).
[44] E. Frumker, G. G. Paulus, H. Niikura, A. Naumov, D. M. Villeneuve, and P. B. Corkum, Opt. Express **20**, 13870 (2012).
[45] A similar double-peaked emission has recently been seen from an autoionization resonance of Sn^+. S. Haessler, V. Strelkov, L. B. E. Bom, M. Khokhlova, O. Gobert, J.-F. Hergott, F. Lepetit, M. Perdrix, T. Ozaki, and P. Salières, New J. Phys. **15**, 013051 (2013).